Quest Journals
Journal of Research in Agriculture and Animal Science Volume 12 ~ Issue 5 (May 2025) pp: 06-16
ISSN(Online) : 2321-9459
www.questjournals.org

Research Paper

Longitudinal Variations of Geomagnetic Field and their Time Derivatives during Ionospheric Disturbance Dynamo over Africa and Asia

Abbas Mustapha[1], Mukhtar Ibrahim Furfuri [2], Mohammed Bello Kaoje [2] Mukhtar Muhammad [3] Asabe A. I[3] Yusuf Aminu Koko[*1] Aminu Mohammad [1*] Yoshikawa Akimoto [4]

[1]*Department of Physics, Kebbi State University of science and Technology, Aliero, Nigeria*
[2]*Federal College of Education Tecgnical, Gusau, Zamfara State, Nigeria*
[3]*Federal University of Agriculture, Zuru, Kebbi State, Nigeria*
[4]*International Center for Space Weather Science and Education (ICSWSE), Kyushu University, JAPAN*

ABSTRACT
In this study, we present and discuss the response of horizontal (H) component of the Earth magnetic field, longitudinal profile during the ionospheric disturbance dynamo (D_{dyn}) and the rate of magnetic field (dH/dt) during 24-25 October 2011 geomagnetic storm in the African and Asian sector. Results revealed that the solar variation SR and the typical H-field at both longitude sectors exhibit higher magnitudes at the equatorial region that the mid-latitudes. At the time of SSC, the typical H-field exhibit higher magnitudes than the solar quiet variation S_R across most of the latitudes in the African sector and only observable in the Asian sector at the mid-latitude. The variation in the intensity of the S_R and the typical H-field during the recovery phase is larger prior to the occurrence of the SSC. The difference could be attributed to the presence of the westward current that manifest as a difference in the typical H-field observed across all the latitudes. Higher rate of magnetic field (dH/dt) are obtain at the time of SSC in the African sector with Asian region exhibiting higher magnitudes during the main phase of the magnetic storm. Generally, both longitude sector show rate of change of magnetic field (dH/dt) during the recovery phase of the magnetic storm which are more noticeable in the African sector This implies that large dH/dt are not only associated to prompt penetration of the magnetospheric electric field (PPEFs) but can also be influenced by ionospheric disturbance dynamo (Dd_{yn}) mechanism.
Keywords: *Magnetosphere; Ionospheric disturbance dynamo; electric field; regular solar variation S_R*

*Received 12 May., 2025; Revised 20 May., 2025; Accepted 22 May., 2025 © The author(s) 2025. Published with open access at **www.questjournas.org***

I. Introduction

It is a well-known fact that current at an altitude range 90 and 120 km in the E-region of the ionosphere is responsible for most of the magnetic field variations at the ground surface. The current is believed to arise from dynamo mechanism [1] in the E-region of the ionosphere. In the absence of solar-terrestrial disturbances, the currents generated through the dynamo process is known as solar quiet or simply 'Sq currents' and their associated fields are solar quiet fields or regular solar daily field variations $S_{R.}$ There are times when the magnetic field exhibit irregular variations caused by different mechanisms such as magnetic storms, resulting to incredible intensification of auroral electrojets that severely alters the global thermospheric circulation. The severity of the disturbance depends on the intensity of the auroral electrojet which in turn depend on several factors that includes magnitude of the storm, local time and location of the station. During this process, two main physical forms of disturbances acting on a global scale have been identified: the direct prompt penetration of the magnetospheric convection electric field (PPEF), [2, 3] and the ionospheric disturbance dynamo process (D_{dyn}), [4]. The disturbance due to prompt penetration of magnetospheric convection electric field on a global scale simultaneously affects the high and low latitudes, [5]. Such magnetic disturbance process was later named disturbance polar 2 (DP2) current systems by [6]. Studies has shown that geomagnetic disturbances at low latitudes are due to prompt penetration of magnetospheric convection electric field which passes through the mid latitude and establish a connection between the high and low latitude region e.g [7, 9]. This influences the electric and magnetic fields at low and equatorial regions. The prompt penetration of magnetospheric convection electric field are generated during the southward/northward turning of the interplanetary magnetic field (IMF) Bz e.g., [10] and is eastward (westward) during the daytime (night-time). Studies also revealed that the enormity of the magnetic storm at the America and Asian sectors causes the magnitude of the DP2 to be higher in these regions over the African sector, [11]. The disturbances in the electric field and current after the main phase of the storm at mid-latitude region are ascribed to ionospheric disturbance dynamo (D_{dyn}) process and manifest at the equatorial region as a decrease on the horizontal (H) component of the Earth magnetic field largely associated with westward current flow.

The (D_{dyn}) is westward (eastward) during the daytime (night-time) hours, [4]. The main signature of the (D_{dyn}) is that it exhibits an eastward current at mid latitude region and westward current at low latitude which is further enhanced with decrease in latitude, [11]. During magnetic storm, large rate of magnetic field (dH/dt) values are major cause of hazards to modern technological systems. Estimate of the dH/dt values provide emergency indices for geomagnetically induce currents (GICs) that poses potential threat to space borne and ground-based conductive infra-structure as well as electrical technological systems. Hence, geomagnetic disturbances may disrupt power transmission network. The scale and magnitude of the damage to a particular network system depends on several factors that include: coordinate system of the site, transmission resistance, topology etc. until now, most of the earlier studies on the ionospheric disturbance dynamo have been basically on the disturbed electric field. [12-16] the neutral wind characterization and simulation with models [4] only few works have been devoted to the identification of disturbance dynamo cases from magnetic field records. Such as the works of [11, 17-20] hence, knowledge on the disturbance dynamo mechanism and the rate of the magnetic field variations which serves as proxy to geomagnetically induce currents remain elusive. This study is set to reveal more morphological features of the Ddyn and the rate of magnetic field during this period so as to ascertain which of the region is at potential risk during times of ionospheric disturbance dynamo mechanism.

II. Observation

Figure 1 shows the index of variability of the interplanetary magnetic field (IMF) Bz, solar wind speed (V_x), interplanetary electric field (IEF), disturbance storm time (D_{st}), Kp index, Au and AL indices respectively. The storm originates from solar flare caused by coronal mass ejection (CME) that hits the Earth and compresses the magnetosphere resulting to sudden storm commencement (SSC) at 18:31 UT on 24th October 2011 marked by a red vertical line as shown in Figure 1 (panel 1a).

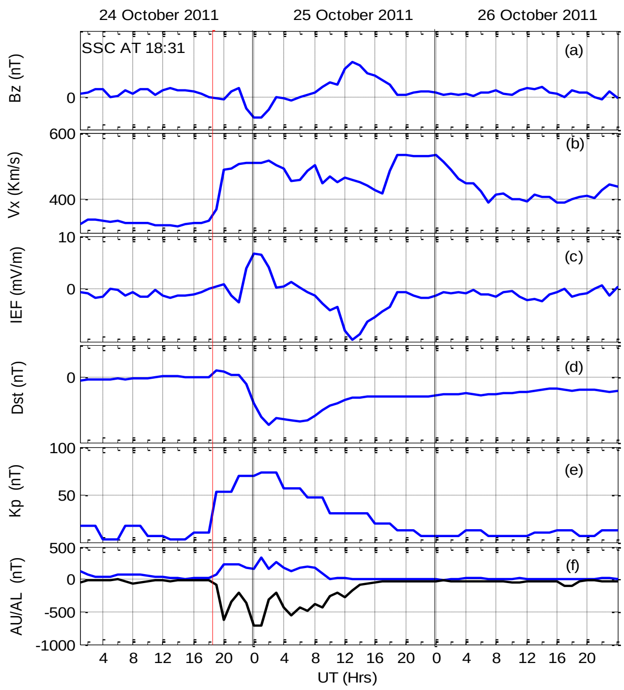

Figure 1 Variations of solar wind parameters on 24-26 October 2011 (a) the Bz component of the interplanetary magnetic field, (b) V_x component of the solar wind, (c) interplanetary electric field (IEF), (d) D_{st} index, (e) Kp index (f) AU (blue) and AL (black) indices.

The initial phase of the storm is marked by a weak southward turning of the (IMF) Bz indicating transfer of energy particles and impulses from solar wind towards the magnetosphere [21, 22]. During the initial phase of the storm, the (IMF) Bz in Figure 1 (panel a) turned northward at 20:00 UT on 24 October 2011 and thereafter it sharply turned southward with a continuous decrease to reach its minimum value ~-18 nT at 01:00 UT seen on 25 October 2011. The northward turning of (IMF) Bz during the initial phase is accompanied by a positive enhancement of Dst index (panel d) which depict the extent of magnetospheric currents, [2]. The minimum Dst value ~-150 nT is seen at 02:30 UT on 25 October 2011 shortly after the minimum (IMF) Bz indication of the magnitude of the magnetospheric current. The interplanetary electric field (IEF) in panel c shows a weak northward magnitude on 24 October 2011 at 18:31 UT with peak value 2.0 mV/m at 20:00 UT. This positive value dropped to a minimum value -4 mV/m at 22:00 UT in total response to the fluctuation of the (IMF) Bz. Maximum positive value of IEF (8 mV/m) occurred around 01:00 UT on 25 October 2011 during the main phase of the storm as depicted by (IMF) Bz. The solar wind speed (V_x) in Figure 1 (panel b) is seen to increase from 320 km/sec to about 520 km/sec in response to the southward turning of the (IMF) Bz. The speed V_x is seen to decrease continuously to ~ 420 Km/sec at 17:00 UT and suddenly increase to 540 Km/sec more than the speed V_x during the initial phase. During the initial phase of the storm, the Kp index (panel e) is about 55 nT and this suddenly increase to ~ 75 nT in response to the southward (IMF) Bz during the main phase indication of a moderate storm. The Kp index shown in Figure 1 (panel e) is also seen to gradually decreases to its minimum value 5 nT at 22:00 UT on 25 October 2011 and fluctuate between 5 and 10 nT through 26 October 2011. The AU and AL indices depict the eastward and westward auroral electrojet currents increase in response to the Joule heating in the auroral zone. Prior to the initial phase of the storm, there were no significant variations in the auroral elctrojet. The occurrence of SSC causes variations of the AU and AL with maximum eastward flow value ~420 nT which correspond to a stronger and oppositely directed (westward) flow with magnitude ~-600 nT observed during the main phase of the storm as shown in Figure 1 (panel f). Variations in AU and AL were also seen during the recovery phase of the storm till 16:00 UT on 25 October 2011, thereafter normal variation is restored.

III. Materials and Methods

2.1 Data Selection and Analysis

The magnetic field records used to achieve the set objective of this work were obtained from the International Real-time Magnetic Observatory Network (INTERMAGNET) and Magnetic Data Acquisition System (MAGDAS) network. The INTERMAGNET and ground-based magnetometer fluxgate of MAGDAS provides one minute values of the Horizontal (H), Declination (D) and Vertical (Z) component of the Earth's magnetic field. However, only the horizontal (H) component of the Earth's main field for 24-25 October, 2011 geomagnetic storm and the average of Five (5) most quiet days before the storm were utilized in the study. The names, locations and magnetic coordinates of the stations used in the study are given in table 1. The days used for the regular solar variation S_R were selected based on the magnetic activity Kp ≤ ±3 downloaded from http:// dx. doi. org/10.1029/JA084iA10p05797 The regular solar variation S_R (quiet reference days) is computed by taking average of five most quiet days in the month for each station under investigation.

Table 1 Geomagnetic coordinates of the Magnetic observatories used in the study

Code	Name	Geographic Latitude	Geographic Longitude	geomagnetic Latitude	geomagnetic Longitude
African Sector					
AAB	Addis Ababa	9.04	38.77	0.18	110.47
ASC	Ascension Island	-7.59	345.62	-2.81	14.36
MBO	M' Bour	14.38	307.27	4.15	14.36
KRT	Khartoum	15.33	32.32	5.69	103.8
NAB	Nairobi	-1.16	36.48	-10.65	108.18
TAM	Tamanrasset	22.79	5.53	13.18	79.7
TSU	Tsumeb	-19.202	17.584	-18.8	17.73
Asian Sector					
TIR	Tirunelveli	8.7	77.8	0.21	149.3
YAP	Yap Island	9.5	138.08	1.49	209.06
CEB	Cebu	10.36	123.91	2.53	195.06

GUA	Guam	13.59	144.7	5.53	144.7
JAI	Jaipur	26.92	75.8	18.35	75.79
KPG	Kupang	-10.2	123.4	-19.58	194.96
KDU	Kakadu	-12.69	132.47	-21.99	-155.22

In a bid to estimate the ionospheric disturbance dynamo (D_{dyn}) we analyze some of the solar wind basic parameters such as interplanetary magnetic field (IMF) Bz which indicate transfer of energy from the solar wind towards the magnetosphere resulting in significant disturbances to the Earth's terrestrial magnetic field. Disturbance storm time (Dst) depict the extent of ring and tail currents caused by magnetospheric disturbances which manifest as a decrease on the horizontal component of the Earth's magnetic field. The negative value of Dst index implies the presence of ring current or both ring and tail currents. The solar wind speed V_x gives estimated amplitudes of the extent of disturbances on solar wind emitted by the sun. The AU and AL are indices which give the measure the eastward and westward auroral electrojet activity. All these solar wind parameters that reveal the characteristic features of the geomagnetic storm were obtained from http://omniweb.gsfc.nasa.gov/form/dx1.html. We also analyzed the horizontal (H) component of the Earth's magnetic field across various latitudes sectors in the Africa and Asian regions. During the recovery phase when auroral activity is weak (<100 nT), the ionospheric disturbance dynamo (D_{dyn}) mechanism as well as the magnetospheric processes are still active creating D_{dyn} and ring current (D_R) responsible for magnetic disturbances. The relationship between these disturbances with the horizontal (H) component of the Earth's magnetic field is given as;

$$D_{dyn} = \Delta H - D_R \cos\gamma - S_R \qquad (1)$$

Where S_R is the regular solar variation, γ is the geomagnetic latitude of the station. ΔH is the horizontal component of the Earth's magnetic field. S_R is used in our study as an average of the five quietest days with Kp $\leq \pm 3$ before the occurrence of magnetic storm and serve as a reference level to depict the extent of deviation of the magnetic field during and after the magnetic storm.

IV. Results

In this paper, we analyzed the behavior of the magnetic field triggered by a geomagnetic storm that occurred on 24 October, 2011 in the Africa and Asian sectors. This is necessary because for each magnetic storm, the ionospheric disturbance dynamo exhibit unique features that differ from one magnetic storm to the other. It is only through series of case identification of ionospheric disturbances that will give us a better understanding of the ionospheric behavior and the physical mechanisms involved during the ionospheric disturbance dynamo which is of uttermost importance during the ionosphere-thermosphere disturbances, GNSS and other communication satellites which are liable to suffer from a number of effects including loss of data, disruption of satellites links, and reduction in the number of available satellites for navigation and positioning [23].

Figure 2 shows the index of variability of the H-field superimposed on the regular solar variation S_R (quiet reference H level) against the universal time over the African sector. The blue line represents the regular solar variation (S_R) and the black line is the typical H-field. It is obvious from Figure 2 that both S_R and the typical H-field exhibit similar occurring pattern that are almost equal in magnitude before the SSC. Similar variation pattern are also observed a day after the magnetic storm (26 October, 2011) but on this day, the difference in magnitude between the S_R and typical H-field is too wide relative to a day before the magnetic storm. This implies that in the absence of any significant magnetic disturbances, the typical H-field and S_R exhibit a regular occurring pattern that are similar both in phase and intensity. The S_R and H-fields both reach their peak almost the same time but appeared earlier (08:00 UT) at AAB then at later time in other latitudes. We clearly observe that at the time of the SSC 18:31 UT on 24th October, 2011, all the stations respond to the direct prompt penetration of the magnetospheres' convection electric field (PPEF). In the African sector, all the stations northward to the magnetic dip equator (see table 1) exhibit positive regular solar variation S_R. Similar positive variation is also seen at the southern hemisphere. The S_R and typical H-field before and after the magnetic storm at AAB closer to the magnetic equator are consistently higher than other stations. Their greater magnitudes reflect direct effect of strong presence of the daytime equatorial electrojet current [24]. The typical H-field is seen to respond to the northward enhancement of the (IMF) Bz during the time of SSC 18:31 UT on 24 October 2011.

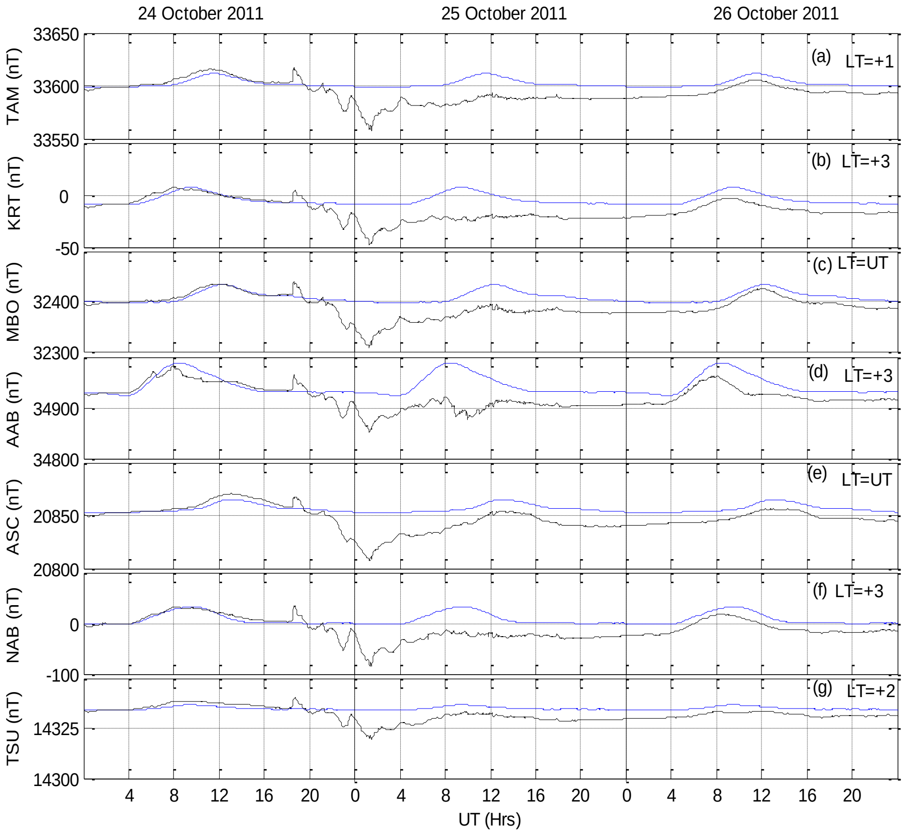

Figure 2 Superimposition of regular solar variation S_R (estimated from the quietest days of H values with Kp ≤ +3) and the typical H-field values for each station plotted with universal time from 24-26 October 2011 in the African sector.

This higher S_R variation at the equatorial region during daytime resulted from cowling conductivity effect at the equatorial altitude with maximum intensity during the daytime. After the magnetic storm, normal S_R does not occur at the same UT hour across the latitudes, rather it occurs 3 hours earlier at AAB. The SSC associated with the compressional state of the magnetosphere and the subsequent transmission of charged particles towards the Earth's surface from the magnetosphere is marked by a sudden impulse at 18:31 UT on 24 October 2011 across all the latitudes followed by a southward disturbance seen also in all the stations which is more noticeable at AAB as shown in Figure 2 (panel d). The severity of the disturbance is weak at low latitude stations (KRT and NAB), as depicted in Figure 2 (panels b and f) then increases afterwards with geomagnetic latitude indication of moving towards its source.

The main phase of the magnetic storm is marked by a step-wise decrease, indication of the westward current flow pattern with minimum peak intensity on 25 October 2011 across all latitudes as depicted by the Dst index in Figure 1 (panel d). The recovery phase shows a gradual variable pattern which is more noticeable at AAB as illustrated in Figure 2. For example, a depression in typical H-field is seen between 08:00-12:00 UT on 25 October 2011 (see Figure 2) simultaneously marked by reduction in IEF and Dst index shown in Figure 1 (panels c and d). The cowling effect which resides at the magnetic equator causes the equatorial electrojet (EEJ) to respond to the fluctuations of the solar wind parameters shown in Figure 1. This southward disturbance of the typical H-field during the recovery phase exhibit signature of the ionospheric disturbance dynamo D_{dyn} that is mainly dominant during the recovery phase of a magnetic storm. The response of the typical H-field after the magnetic storm shows a decrease in amplitude with respect to S_R. The difference in the peak amplitude is larger in AAB with value up to ~45 nT around 08:00 UT on the 26 October 2011. Other stations also show similar difference with less magnitude compared to the one seen at AAB. This difference is as a result of westward current (ring current) superimposed on the eastward current and manifest as a decrease in typical H-field observed across all latitudes.

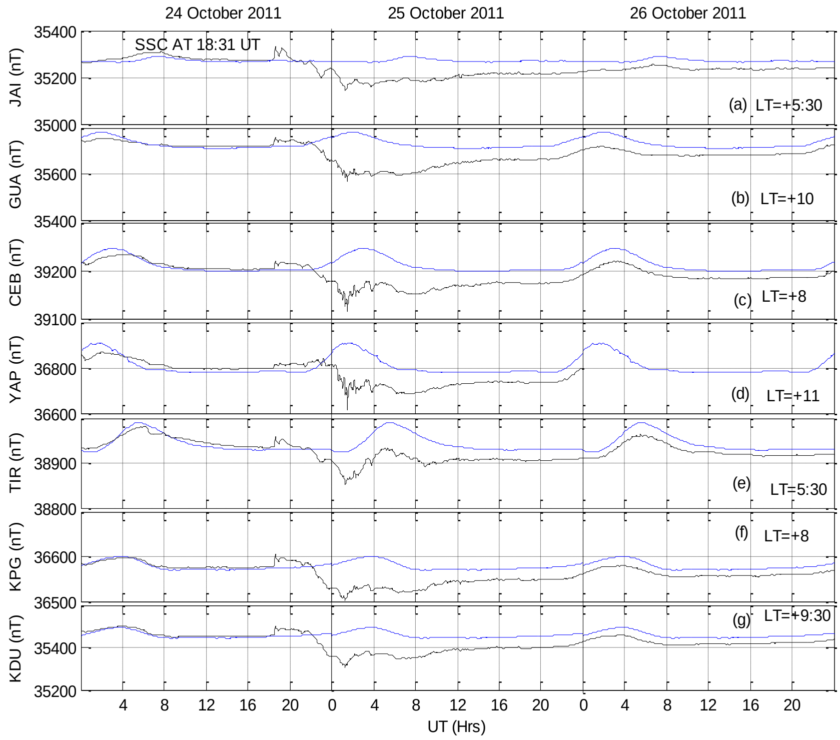

Figure 3 Superimposition of regular solar variation S_R (estimated from the quietest days of H values with Kp≤+3) and the typical H-field values for each station plotted with universal time from 24-26 October 2011 in the Asian sector.

As seen in Figure 3, the response of the typical H-field at the equatorial stations during the SSC in relation to the regular solar variation S_R is similar to the African sector. The daytime S_R is conspicuously seen to be higher than the SSC at the equatorial stations (JAI and KDU) and reverse is the case at other latitudes stations as shown in Figure 3. At the time of the SSC (18:31 UT) both longitudes (Asia and Africa) sector are in the local dusk-dawn sector characterized with a weak E-region conductivity, hence we assert that there could be injection of other mechanisms that enhanced the S_R more than the magnitude of the Chapman-Ferraro current associated with the SSC. After storm main phase, the typical H-field steadily recovers that appears faster at TIR and YAP latitudes and slower at other latitudes which demonstrates evidence of longitudinal variations in geomagnetic activity. Just like the African sector, the difference in the magnitude of the S_R and typical H-field are larger during the recovery phase prior to the occurrence of the SSC in the Asian sector. This again justifies the effect of the westward current generated by ionospheric disturbance dynamo mechanism [17, 18, 25, and 26]. A depression is observed during the recovery phase across all latitudes in the Asian sector on 25 October 2011 between 06:00-12:00 UT similar to the one seen at AAB on the same day around 08:00-1200 UT. This depression appeared earlier in the Asian sector to the African sector. This signature is a clear demonstration of the longitudinal inequality of the ionospheric disturbance dynamo mechanism [18, 19, 24].

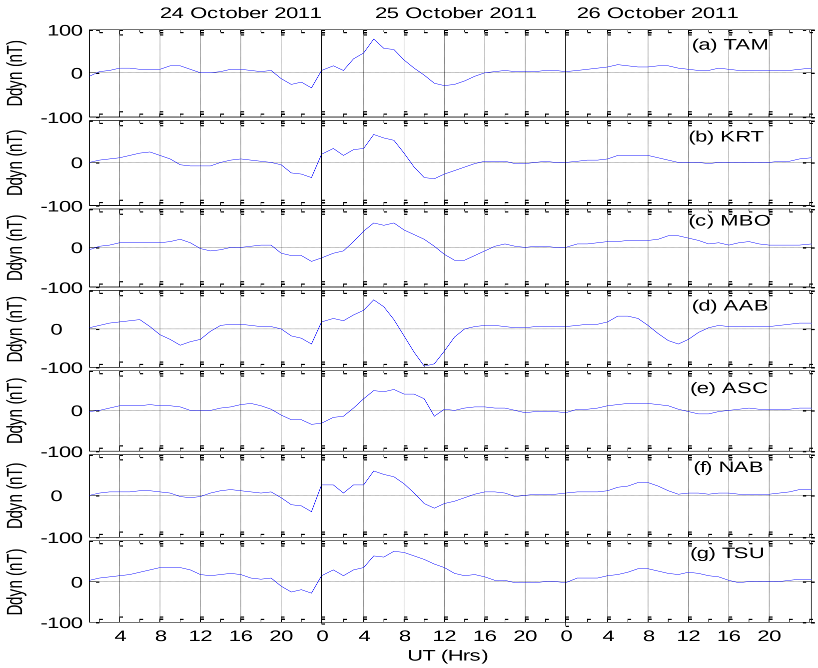

Figure 4 Latitudinal variation of the D_{dyn} disturbance in the African sector

Figure 4 shows the latitudinal variation of the ionospheric disturbance dynamo (D_{dyn}) against universal time (UT) over the African sector. It is obvious that during the SSC, the ionospheric disturbance dynamo D_{dyn} exhibit southward direction around (19:00-00:00) UT on 24 October, 2011 across all the latitudes in the African sector with similar features but only at KDU and KPG latitudes in the Asian sector as demonstrated in Figure 5. During these periods, (19:00-00:00) UT the D_{dyn} generates westward magnetic field variations which is the typical signatures of the ionospheric disturbance dynamo mechanism [26]. The westward magnetic field is due to the westward current generated by the D_{dyn} process that superimposed the eastward current. The positive D_{dyn} enhancement observed around (19:00-00:00) UT could be induced by the Chapman-Ferraro current.

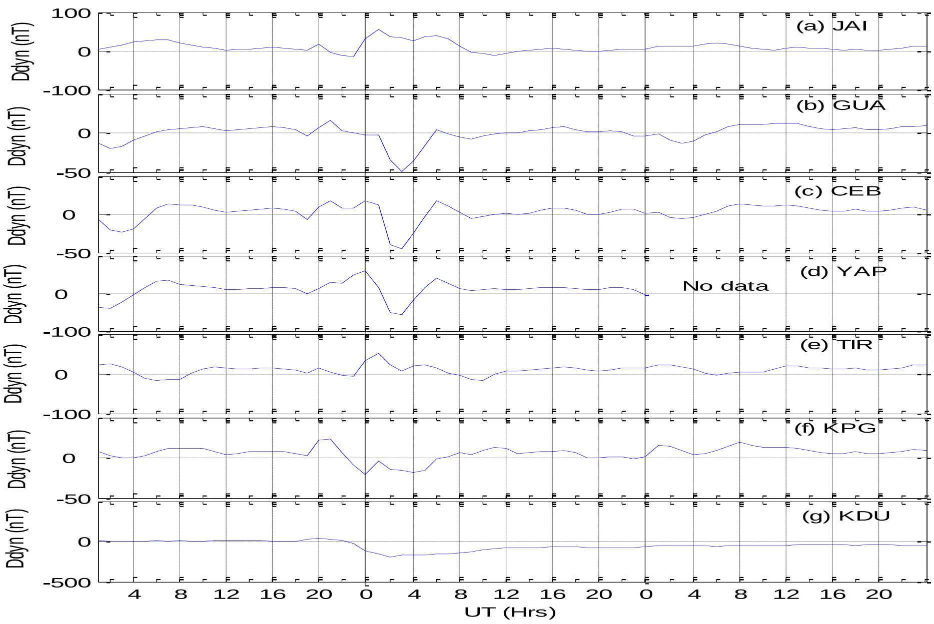

Figure 5 Latitudinal variation of the D_{dyn} disturbance in the Asian sector

Figure 6a and 6b show the time derivative of the Earth's magnetic field against universal time (UT) in the African sector. It is obvious that the magnitude of dH/dt at the time of the SSC is higher than during the main and recovery phase of the magnetic storm in consistence with the earlier studies by [25]. These authors observed higher rate of magnetic field during the storm sudden commencement at low-latitude in China. AAB closer to the magnetic dip equator exhibit higher dH/dt with peak amplitude 19 nT/s closely followed by a low latitude station, ASC (panel e) with peak amplitude 15 nT/s.

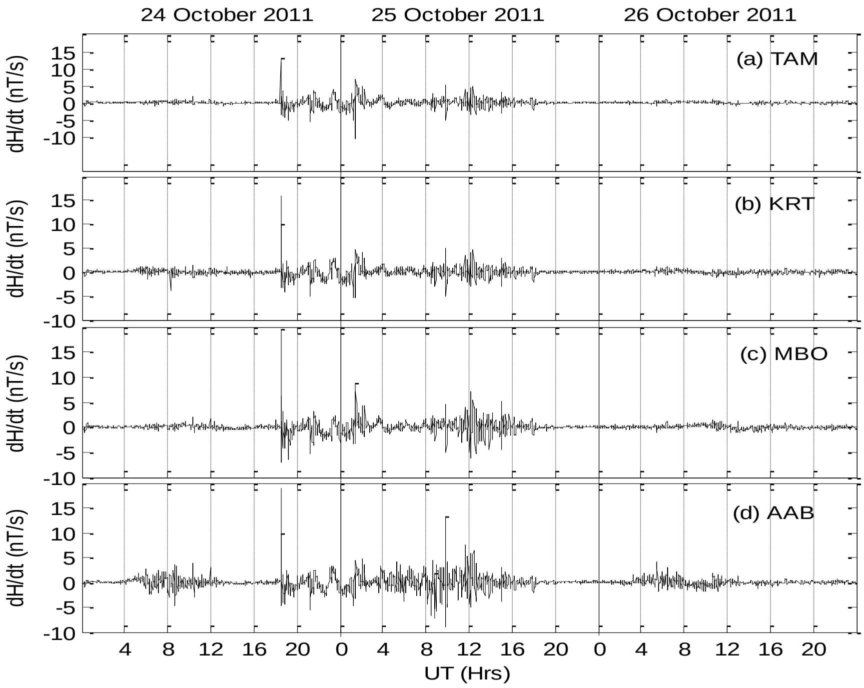

Figure 6a Rate of change of magnetic field in the African sector

Other stations also show similar enhancement but much smaller to the ones on the equatorial-low latitude region. This implies that equatorial electrojet plays significant role in enhancing magnetic variations within the equatorial low latitude. The magnitude of the rate of magnetic field is higher at the time of SSC (18:31 UT) in the African sector which by extension, higher geomagnetically induced current (GICs) may likely occur during the SSC of this magnetic storm [25, 26] contrary to the Asian sector with maximum dH/dt during the main phase of the magnetic storm as depicted in Figure 7 (panels c, d and e).

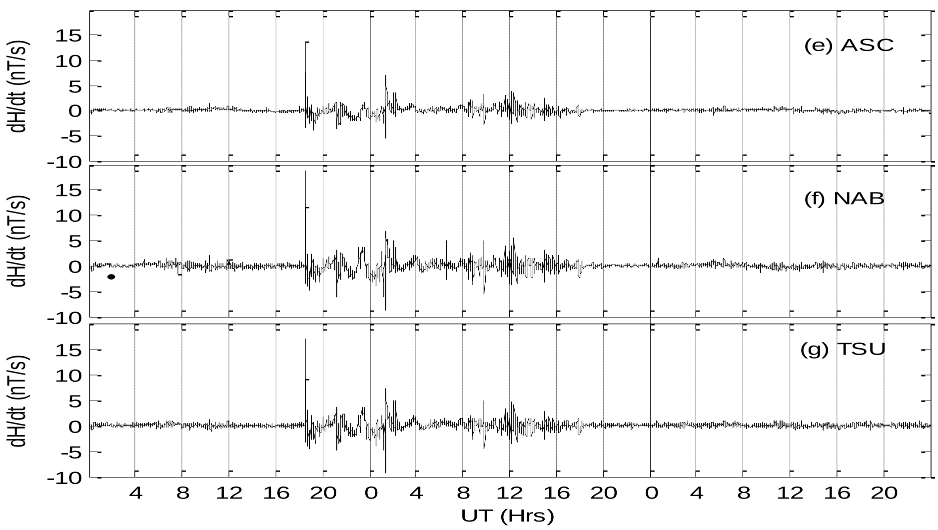

Figure 6b continues for rate of change of magnetic field in the African sector.

This implies that higher GICs values are likely to occur during the main phase of the magnetic storm in these regions. The rate of magnetic field variation observed in Figure 7 (panel a) at GUA does not give good representation of a geomagnetic storm. From Figure 6b and 6b, it is also clear that the rate of change of magnetic field is not only limited to the period of SSC and main phase of a magnetic storm, it thus indicate that during recovery phase which is known to be dominated by the ionospheric disturbance dynamo process can also influence large rate of magnetic field (dH/dt).

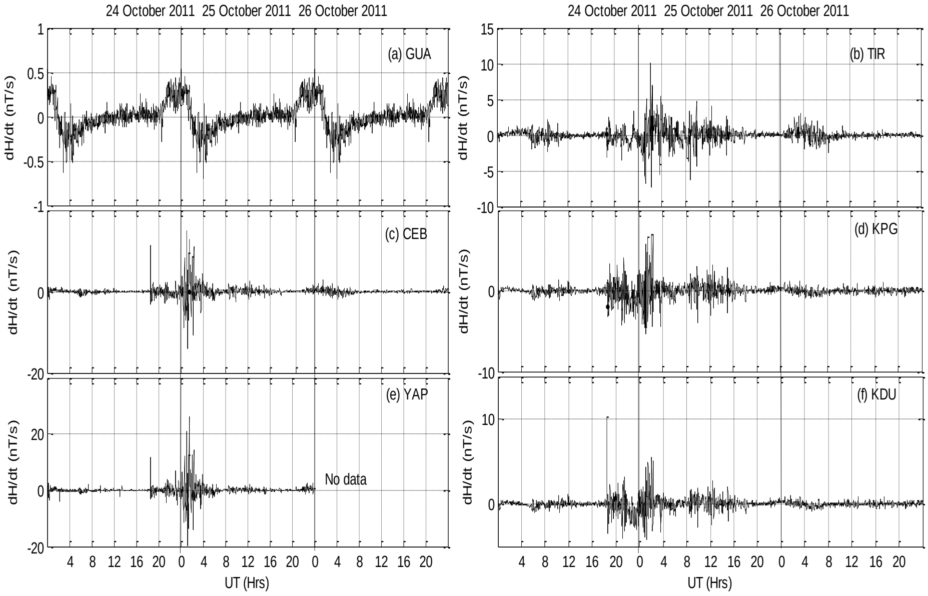

Figure 7 Rate of change of magnetic field in the Asian sector

At AAB in Figure 6a (panel d) large value of dH/dt up to -9 nT/s is seen on 25 October 2011 around 10:00 UT during the recovery period which is higher than the value -3 nT/s observe during the main phase of the magnetic storm. Other stations also show similar enhancement during the recovery phase. This shows that large dH/dt are not only associated to the prompt penetration of the magnetospheric convection electric field but can as well be influenced by the D_{dyn} electric field.

V. Conclusions

Using magnetic field records from the INTERMAGNET and MAGDAS network we present features of the ionospheric disturbance dynamo and the rate of change of magnetic field (dH/dt) along the Africa and Asian sector during 24-25 October 2011 geomagnetic storms. Some of the salient features observed during the study are summarized below:

1. During the SSC, the typical H-field shows higher magnitudes than the SR across all the latitudes in the African sector exception of AAB that lies along the magnetic equator, while reverse is the case in the Asian sector with exception of JAI and KDU with higher H-field magnitudes. At the time of the SSC (18:31 UT) both longitudes sector are in the local dusk-dawn sector characterized with a weak E-region conductivity hence may likely be a factor responsible for the lesser SSC amplitude to the daytime S_R in the two longitude sector

2. Large differences exist between the SR and the typical H-field during the recovery phase compare to their difference before the occurrence of the SSC. This large different may be resultant effect of the westward current generated by the ionospheric disturbance current during the recovery phase of the magnetic storm
3. For this magnetic storm, higher rate of change of magnetic field (dH/dt) are obtained at the time of SSC in the African sector with Asian region exhibiting higher variations during the main phase of the magnetic storm.

4. Generally, both longitude sector show rate of change of magnetic field (dH/dt) during the recovery phase of the magnetic storm which are more noticeable in the African sector. This implies that large dH/dt are not only associated to the prompt penetration of magnetospheric electric field which are dominant during the main phase of a magnetic storm but can as well be influence by D_{dyn} electric field during the recovery phase.

.**Author Contributions**

The conceptualization of the work was done by Mustapha Abbas and the methodology was designed by Mustapha Abbas and Mukhtar Ibrahim Furfuri. The data arrangement was done by Asabe Audu Ibrahim. The software application was carried out by Mohammed Bello Kaoje, and Mukhrat Mohammed and the validation

was done by Aminu Mohammed and Aminu Yusuf Koko. The First draft copy of the manuscript was prepared by Mustapha Abbas, reviewed by Yoshikawa Akimoto.
All authors have read and agreed to the published version of the manuscript.

Funding

This work received no external funding.

Acknowledgments

The authors acknowledge all of MAGDAS hosts for maintaining our instrument whose magnetic field records are used in this study.

Conflicts of Interest

The authors declare no conflict of interest.

References

[1] Chapman, S. (1919). I. The solar and lunar diurnal variations of terrestrial magnetism. Phil. Trans. R. Soc. Lond. A, 218(561-569), 1-118, https://doi.org/10.1098/rsta.1919.0001.

[2] Vasyliunas, V. M. Mathematical models of the magnetospheric convection and its coupling to the ionosphere, in Particles and Fields in the Magnetosphere, edited by M. mcCormac, pp. 60-71, Springer, New-York, doi:10.1007/978-94-010-3284-1-6, 1970.

[3] VasyliunasV, M. (1972). The interrelationship of magnetospheric processes, in Earth's M agnetospheric processes', edited by B. M. McCormac, pp. 29-38, D. Reidel, Norwell, Mass.

[4] Blanc, M., and Richmond A. D. (1980). The ionospheric disturbance dynamo, J. Geophys. Res., 85, 1669. https://doi.org/10.1029/JA085iA04p01669

[5] Nishida, A., N. Iwasaki, and N. T. Nagata. (1966). The origin of fluctuations in the equatorial electrojet: A new type of geomagnetic variation, Ann. Geophys., 22, 478–484.

[6] Nishida, A (1968). Geomagnetic DP2 fluctuations and associated phenomena, J. Geophys. Res., 73, 1795–1803, https://doi.org/10.1029/JA073i005p01795.

[7] Reddy, C. A., Somayajulu , V. V and Devasia, C. V. (1979). Global scale electrodynamics coupling of the auroral and equatorial d dynamo regions, J. Atmos. Terr. Phys., 29, 187, https://doi.org/10.1016/0021-9169(79)90012-6

[8] Kikuchi, T., Liihr, H, Kitamura, T, Saka, O, and Schlegel, K. (1996). Direct penetration of the polar electric field to the equator during a DP 2 event as detected by the auroral and equatorial magnetometer chainsa nd the EISCAT radar, J. Geophys. Res https://doi.org/10.1029/96JA01299.

[9] Kobea, A. T., C. A. Mazaudier, J. M. Do, H. Liihr, E. Houngninou J, . Vassal,E . Blanc,a nd J. J. Curto (1998). Equatorial electrojet as part of the global circuit: A case study from the IEEY, Ann. Geophys., 16, 698-710, https://doi.org/10.1007/s00585-998-0698-1

[10] Sastri, J. H, Abdu, M. A, and Sobral, J. H. A. (1997). Response of equatorial ionosphere to episode of asymmetric ring current activity. Ann. Gephys., 15, 1316-1323, https://doi.org/10.1007/s00585-997-1316-3

[11] Zaka, K. Z., A. T. Kobea, A. T, Assamoi, P, Obrou, K, O, Doumbia, V, Boka, K, Adohi, B. P. J and Mene, N, M.(2009). Latitudinal profile of the ionospheric disturbance dynamo magnetic signature comparison with DP2 magnetic disturbance, Ann. Geophys., 27, 3523–3536, https://doi.org/10.5194/angeo-27-3523-2009

[12] Fejer, B. G.,Larsen, M. F and Farley, D, T. (1983). Equatorial disturbance dynamo electric fields, Geophys. Res. Lett., 10, 5337±5340, https://doi.org/10.1029/GL010i007p00537

[13] Spiro, R. W., Wolf, R, A, and Fejer, B, G. (1988). Penetration of high- latitude electric field effects to low latitudes during SUNDIAL 1984, Ann. Geophysicae., 6, 39±50.

[14] Sastri, J. H. (1988). Equatorial electric fields of ionospheric disturbance dynamo origin, Ann. Geophysicae., 6, 635±642, http://hdl.handle.net/2248/3711

[15] Fejer, B. G., Spiro., R. G, Wolf, A., R, and Foster, J. G. (1990a). Latitudinal variations of perturbation electric fields during magnetically disturbed periods: 1986 SUNDIAL observations and model results, Ann. Geophysicae., 8, 441±454

[16] Huang, C.-S, Foster, J. C. and Kelley, M. C. (2005a). Long-duration penetration of the interplanetary electric field to the low-latitude ionosphere during the main phase of magnetic storms, J. Geophys., Res., 110, A11309, https://doi.org/10.1029/2005JA011202

[17] Le Huy, M., and Amory-Mazaudier. C. (2005). Magnetic signature of the ionospheric disturbance dynamo at equatorial latitudes: "Ddyn", J. Geophys. Res., 110, A10301, https://doi.org/10.1029/2004JA010578

[18] Le Huy, M., and Amory-Mazaudier , C. (2008). Planetary magnetic signature of the storm wind disturbance dynamo currents: Ddyn, J. Geophys. Res., 113, A02312, https://doi.org/10.1029/2007JA012686

[19] Zaka, K. Z., et al. (2010). Simulation of electric field and current during the 11 June 1993 disturbance dynamo event: Comparison with the observations, J. Geophys. Res., 115, A12314, https://doi.org/10.1029/2010JA015417

[20] Shimeis, A., I. Fathy, Amory-Mazaudier, C, Fleury, R, Mahrous, A. M. A. Yoshikawa, A, and Groves K.(2010). Signature of the coronal near the northcrest equatorial anomaly over Egypt during the strong geomagnetic storm 5 April 2010, J. Geophys. Res., 117, A07309, https://doi.org/10.1029/2012JA017753

[21] Imitiaz, N, Younas, W and Khan, M. (2020). Response of the low- to mid-latitude ionosphere to the geomagnetic storm of September 2017. Ann. Geophys., 38, 359–372, https://doi.org/10.5194/angeo-38-359-2020,

[22] Astafyeva, E., Zakharenkova, I., Hozumi, K., Alken, P., Coïsson, P., Hairston, M. R., & Coley, W. R. (2018). Study of the equatorial and low-latitude electrodynamic and ionospheric disturbances during the 22–23 June 2015 geomagnetic storm using ground-based and spaceborne techniques. Journal of Geophysical Research: Space Physics, 123, 2424–2440, https://doi.org/10.1002/2017JA024981

[23] Abbas, M., Abidin, Z.Z., Jusoh, M.H, Bolaji, O. S, and Yoshikawa, A. (2019). Features of horizontal magnetic field intensity over northern island of Malaysia. *Indian J Phys* **93**, 1247–1257, https: //doi. org/10 .1007/s 12648-019-01388-9.

[24] Fathy, I., C. Amory-Mazaudier, A. Fathy, A. M. Mahrous, K. Yumoto, and E. (2014). Ghamry Ionospheric disturbance dynamo associated to a coronal hole: Case study of 5–10 April 2010, J. Geophys. Res. Space Physics, 119, 4120–4133, https://doi.org/10.1002/2013JA019510

[25] Zhang, J. J., Wang, C, Sun, T, R, Liu, C. M, and Wang , K. R. (2015). GIC due to storm sudden commencement in low-latitude high-voltage power network in China: Observation and simulation, *Space Weather*, *13*, https:// doi. org/ 10.1002/2015SW001263

[26] Ngwira, C. M, McKinnell, L-A, and Prierre, J. C. (2011). Geomagnetic activity indicators for geomagnetically induced current studies in South Africa. Adv., Space, Res., 48, 529-534, 2011. https ://doi. org/10. 1016/j .asr. 2011 .03.042